# Dynamics of phase separation in block copolymer melts

Fong Liu and Nigel Goldenfeld
*Department of Physics and Materials Research Laboratory, University of Illinois at Urbana-Champaign, Urbana, Illinois 61801*
(Received 19 December 1988)

We consider the partial differential equation which describes phase separation in a block copolymer melt. We construct numerically the periodic solution which minimizes the free energy. The lamellar thickness of the final equilibrium pattern is found to scale with the molecular weight as a power law $\lambda_L \sim N^{\theta}$. The exponent $\theta$ takes the value $\frac{1}{2}$ in the weak-segregation regime and $\frac{2}{3}$ in the strong-segregation regime. We propose a scaling theory of the dynamics, from which we obtain $\theta=2\phi$, where $\phi$ is the scaling exponent in spinodal decomposition, in agreement with a conjecture by Oono and Bahiana [Phys. Rev. Lett. **61**, 1109 (1988)]. Lastly, we also study the pattern formed by propagating fronts. The selection of the unique velocity of the front and of the wavelength of the pattern behind the front agrees well with the marginal-stability theory.

## I. INTRODUCTION

When a homogeneous binary system in its high-temperature stable phase is quenched rapidly below its critical temperature, phase separation occurs. The system will eventually phase separate into its two stable states through either spinodal decomposition or nucleation. In spinodal decomposition, after the system is quenched, initial microscopic fluctuations grow in magnitude and develop a pattern with a single characteristic length scale $l(t)$. It has been established that in the late stages of phase separation, the variation of the length scale with time obeys a power law, $l(t)\sim t^{\phi}$. Consequently, the scattering form factor also adopts a universal scaling form.[1] These scaling laws are now well established, and have been extensively studied[2] by both real and computer experiments, as well as analytical calculations. The value of the exponent $\phi$ depends on whether or not the order parameter, which in a binary alloy is taken to be the density difference between the two components, is conserved. In the conserved case, there is strong evidence that the exponent $\phi=\frac{1}{3}$, while in the nonconserved case, it is believed that $\phi=\frac{1}{2}$.[1-3] These results do not appear to depend on the dimensionality of the system.

In a block copolymer (BCP) melt, the phase separation process proceeds differently. A block copolymer is a linear chain molecule consisting of two covalently bonded monomer units $A$ and $B$. In the copolymer melt above the critical temperature $T_c$, $A$ and $B$ mix. Below $T_c$, when the two sequences are incompatible with each other, the copolymer melt undergoes phase separation. However, spinodal decomposition cannot occur because the two monomer sequences are chemically bonded, and thus cannot separate indefinitely. As a result, the phase separation occurs on a mesoscopic scale where banded microdomains of $A$-rich and $B$-rich regions emerge in the final equilibrium state.

Experimentally, ordered periodic lamellar, cylindrical or spherical structures have been observed.[4] The period $\lambda_L$ of the lamellar structure is found to scale as a power law with the polymerization index $N$, i.e., $\lambda_L \sim N^{\theta}$. In the so-called weak-segregation regime, where the thickness $\xi$ of the interface between the $A$-rich and $B$-rich phase is comparable to $\lambda_L$, the exponent $\theta_w=\frac{1}{2}$, while in the strong-segregation regime, where $\xi \ll \lambda_L$, $\theta_s=\frac{2}{3}$.[5]

Ohta and Kawasaki[6] have studied this system using a variational method. They minimized the Landau free energy given by Leibler,[7] and by assuming a certain form for the trial order parameter, they obtained the exponents mentioned above. Oono and Shiwa[8] later proposed to model the BCP system by a computationally efficient cell dynamical system method,[3] which models the time evolution of the system on a discrete space-time lattice by injective map dynamics. In two dimensions, the cell dynamical system approach has been pursued by Oono and Bahiana,[9] who confirm that the weak-segregation exponent $\theta_w=\frac{1}{2}$. Unfortunately, they cannot reach the more interesting strong-segregation regime, being limited by the huge computation time requirement. However, they argue, by dimensional analysis, that the $\frac{1}{3}$ strong-segregation exponent is exact and, moreover, that the BCP exponent $\theta$ is related to the spinodal exponent $\phi$ through the relation $\theta=2\phi$.

The purpose of this paper is to analyze pattern formation in block copolymer melts from the more traditional formulation using partial differential equations. The dynamical equation describing phase separation in block copolymer melts is a modification of the Cahn-Hilliard equation. We show that this equation possesses a family of periodic lamellar states. By minimizing the Lyapunov free-energy functional we are able to select a state with minimum free energy which physically corresponds to the lamellar pattern observed in block copolymer experiments. We confirm the scaling relation $\lambda_L \sim N^{\theta}$ and demonstrate the crossover from a weak-segregation exponent of $\theta_w=\frac{1}{2}$ to a strong-segregation exponent $\theta_s=\frac{2}{3}$. A scaling form for the length scale as a function of time and polymerization index is also proposed that leads naturally to the conclusion $\theta=2\phi$. This work is described in Sec. II of this paper.

 

These considerations apply when the system reaches thermodynamic equilibrium. In practice, this might take a long time to attain, and so we also discuss how lamellar states can be formed far from equilibrium, behind a front propagating into the thermodynamically unstable state. Apart from its intrinsic experimental relevance, this mechanism for pattern formation is of interest because the linearized BCP equation can be cast in the same form as the linearized Swift-Hohenberg equation,[10] which models Rayleigh-Bénard convection.[11] Our numerical simulations of front propagation show that the speed and characteristic wavelength of the front are the same in both cases, and are correctly predicted by the marginal-stability hypothesis,[12] even though the Swift-Hohenberg and the block copolymer equations have different nonlinear terms. This work is described in Sec. III.

## II. LAMELLAR PATTERN SELECTION IN EQUILIBRIUM

### A. Modeling and equilibrium states

The dynamics of phase separation in a block copolymer melt is described by the partial differential equation in space $\mathbf{r}$ and time $t$:[8]

$$\frac{\partial\psi(\mathbf{r},t)}{\partial t}=L\nabla^2(-\tau\psi+\mu\psi^3-\nabla^2\psi)-\epsilon(\psi-1+2f)\ , \quad (2.1)$$

where $f\in(0,1)$ is the molecular weight ratio of the $A$ monomer. $\psi(\mathbf{r},t)$ is the scalar order parameter chosen to be $(1-f)\rho_A-f\rho_B$, where $\rho_A$ and $\rho_B$ are reduced local monomer densities. $\psi$ is identically zero in the high-temperature homogeneous phase and nonzero in the low-temperature phase-separated phase. $L$ is the mobility and $\mu$ is a positive phenomenological constant. $\tau$ is a phenomenological parameter characterizing $A$-,$B$-monomer interaction. Below some critical temperature $T_c$, $\tau$ becomes positive and monomers tend to phase separate. Later we will see that $\tau$ is related to the Flory-Huggins parameter. The polymerization index $N$ enters the equation through the small parameter $\epsilon$, which is proportional to $N^{-2}$. In this paper, we will mainly report on the case of 1:1 even block copolymers where $f=\frac{1}{2}$. The case of uneven length $f\neq\frac{1}{2}$ will be mentioned briefly. We will refer to Eq. (2.1) as the BCP equation below. In principle, there is also a stochastic contribution which should be added to Eq. (2.1) to ensure that thermal equilibrium can be attained as $t\to\infty$.

Setting $\epsilon=0$ in Eq. (2.1) we recover the well-known Cahn-Hilliard equation. In one dimension, the Cahn-Hilliard equation admits a one-parameter continuous family of steady-state periodic solutions, and a limiting nonperiodic tanh-like solution. None of these periodic solutions are minima of the free energy and thus are not admissible as $t\to\infty$. Instead, the asymptotic state is the nonperiodic tanh-like solution which attains the global minimum of the free energy.

Equation (2.1) is in some sense the simplest modification of the Cah-Hilliard equation which describes the formation of lamellar patterns. As we shall show, adding the term proportional to $\epsilon$ makes the state $\psi=0$ more stable than the $\psi\neq0$ state, in the absence of a spatial gradient. A consequence is the existence of a periodic equilibrium pattern which minimizes the free energy. The singular nature of this additional term can be seen by making a change of scale $\mathbf{r}'=\epsilon^{1/2}\mathbf{r}$, $t'=\epsilon t$. Equation (2.1) becomes

$$\frac{\partial\psi(\mathbf{r},t)}{\partial t}=-\epsilon\nabla^4\psi+\nabla^2(-\psi+\psi^3)-\psi\ , \quad (2.2)$$

where we have omitted primes and without loss of generality set $L,\tau,\mu$ to 1 and $f=\frac{1}{2}$ for simplicity. The singular nature of the $\epsilon$ term arises because it is the coefficient of the highest derivative in Eq. (2.2).

Equation (2.2) can be derived from a Ginzburg-Landau free energy, using the phenomenological time-dependent Ginzburg-Landau equation for a conserved order parameter

$$\frac{\partial\psi(\mathbf{r},t)}{\partial t}=\nabla^2\frac{\delta F\{\psi(\mathbf{r},t)\}}{\delta\psi(\mathbf{r},t)}\ , \quad (2.3)$$

where

$$F\{\psi\}=\frac{1}{V}\int_V\left[\frac{\epsilon}{2}(\nabla\psi)^2-\frac{\psi^2}{2}+\frac{\psi^4}{4}\right]d\mathbf{r}+\frac{1}{2V}\int_V\int_V G(\mathbf{r},\mathbf{r}')\psi(\mathbf{r},t)\psi(\mathbf{r}',t)d\mathbf{r}\,d\mathbf{r}'\ , \quad (2.4)$$

and $G$ is the Green's function for Laplace's equation

$$\nabla^2G(\mathbf{r},\mathbf{r}')=-\delta(\mathbf{r}-\mathbf{r}')\ , \quad (2.5)$$

with appropriate boundary conditions. The free-energy equation (2.4) is essentially the effective Hamiltonian first derived by Leibler[7] and discussed by Ohta and Kawasaki[6] for a block copolymer system. We can relate parameter $\tau$ in Eq. (2.1) to the Flory-Huggins parameter $\chi$ through[6]

$$\tau=8f(1-f)\rho_0\chi-\frac{2s(f)}{f(1-f)N}\ ,$$

where $\rho_0$ is the monomer number density and $s(f)$ is a constant of order unity. The second term in $F$ represents the long-range interaction of $\psi(\mathbf{r})$ due to the connectivity of different chemical sequences in a copolymer chain. It is the presence of both short-range and long-range interactions which allows the existence of equilibrium periodic states.

We note also that $F\{\psi\}$ acts as a Lyapunov functional, since

$$\frac{\partial F\{\psi(\mathbf{r},t)\}}{\partial t}\leq0\ .$$

Since we are primarily interested in modeling the quasi-one-dimensional periodic lamellar patterns observed in BCP experiments, it suffices to focus on a one-dimensional version of Eq. (2.2). As we show below, for $0<\epsilon\leq\frac{1}{4}$, Eq. (2.2) has a one-parameter continuous family of periodic steady-state solutions. The experimentally observed lamellar pattern corresponds to the one with the lowest free energy.

We now discuss the periodic solutions of Eq. (2.2) in detail. These solutions emerge as the homogeneous $\psi=0$ solution of Eq. (2.2) loses its stability. Consider infinitesimal perturbations of the form $e^{\omega t+ikr}$ around the $\psi=0$ state. The linear dispersion relation is given by

$$\omega(k)=-\epsilon k^4+k^2-1 \ . \tag{2.6}$$

The $\psi=0$ state becomes linearly unstable when $0<\epsilon\leq\frac{1}{4}$. Meanwhile, periodic solutions appear with wavelength $\lambda=2\pi/k$ bounded by $\lambda\in[\lambda_2,\lambda_1]$, where

$$\lambda_{1,2}=\sqrt{2}\pi(1\pm\sqrt{1-4\epsilon})^{1/2} \ . \tag{2.7}$$

The neutral stability curve, obtained by setting $\omega(k_{1,2})=0$ in the dispersion relation, is plotted in Fig. 1.

To find the periodic solutions numerically, an arbitrary $\lambda$ is chosen first and Eq. (2.2) is evenly discretized over length $[0,\lambda/2]$. Equation (2.2) is then iterated using Newton's relaxation algorithm (IMSL routine BVPFD) with boundary conditions $d\psi(r)/dr=d^3\psi(r)/dr^3=0$ at $r=0,\lambda/2$. We usually start the iteration from an initial profile $\psi(r)=\cos(2\pi r/\lambda)$, and convergence to the final states is found to be rapid. We verified that the final state is independent of the exact form of the initial conditions. If a solution exists for a particular $\lambda$, it is reached quite efficiently and accurately. We normally use $\sim$250 grid points in the discretization to ensure a relative accuracy of $10^{-6}$ in $\psi$.

For each $\epsilon\in(0,\frac{1}{4})$, we indeed obtain a periodic solution for all $\lambda$ lying within the neutral stability boundaries. The amplitude of the solution increases from zero as we move inward from the neutral stability curves, and attains a maximum somewhere between the two curves. At a given $\lambda$, the profile of the solution is cosine-like for large $\epsilon$ and rather square-wave-like for small $\epsilon$ (Fig. 1, inset).

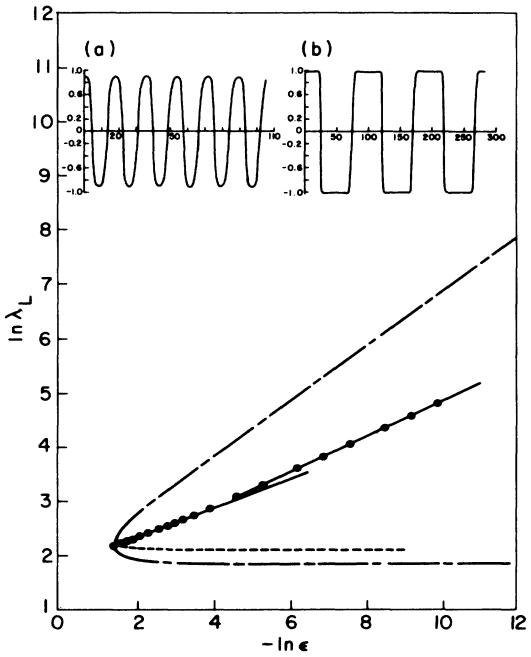


FIG. 1. Lamellar thickness $\lambda_L$ of the final equilibrium pattern as a function of $\epsilon$. The chain-dashed line is the neutral stability curve; the dashed line, the wavelength selected by propagating fronts. Solid lines have slopes 0.263 and 0.325. Insets are order parameter profiles for (a) $\epsilon=0.02$ and (b) $\epsilon=1.0\times10^{-4}$.

### B. Pattern selection by free-energy minimization

The periodic solution with lowest free energy can be found explicitly from Eq. (2.4). Using the symmetry and conservation properties of $\psi(r)$,

$$\int_0^{\lambda}\psi(r)dr=0, \quad \psi(r)=\psi(r+\lambda)=\psi(-r) \ ,$$

and choosing $G(r-r')=-|r-r'|/2$, Eq. (2.4) can be written in terms of integrals over a half period $\lambda/2$:

$$F_\lambda\{\psi\}=\frac{2}{\lambda}\int_0^{\lambda/2}\left[\frac{\epsilon}{2}\left[\frac{d\psi}{dr}\right]^2-\tfrac{1}{2}\psi^2+\tfrac{1}{4}\psi^4\right]dr - \frac{1}{2\lambda}\int_0^{\lambda/2}\int_0^{\lambda/2}|r-r'|\psi(r)\psi(r')dr\,dr' \ . \tag{2.8}$$

Special symmetry properties of the $f=\frac{1}{2}$ even block copolymer case allow the further reduction of Eq. (2.8) to integrals over $\frac{1}{4}$ of a period,

$$F_\lambda\{\psi\}=\frac{4}{\lambda}\int_0^{\lambda/4}\left[\frac{\epsilon}{2}\left[\frac{d\psi}{dr}\right]^2-\tfrac{1}{2}\psi^2+\tfrac{1}{4}\psi^4\right]dr-\frac{1}{\lambda}\int_0^{\lambda/4}\int_0^{\lambda/4}\left[|r-r'|+r+r'-\frac{\lambda}{2}\right]\psi(r)\psi(r')dr\,dr' \ . \tag{2.9}$$

We evaluate Eq. (2.9) numerically with the previously found steady states using IMSL interpolation and integration routines BS2IN and BS2IG. For a given $\epsilon$, all steady states are found to have negative free energies, i.e., they are more stable than the homogeneous $\psi=0$ state. We then minimize $F_\lambda$ with respect to $\lambda$. We find that $F_\lambda$ attains its minimum value at a single wavelength $\lambda^*\in[\lambda_2,\lambda_1]$. Finally, returning to unscaled variables, the lamellar thickness $\lambda_L$ is given by $\lambda_L=\epsilon^{-1/2}\lambda^*$.

In Fig. 1 is shown the log-log plot of equilibrium lamellar thickness $\lambda_L$ as a function of $\epsilon$. Also included in the figure are the neutral stability curve and a curve giving the lamellar thickness obtained from the propagating front mechanism discussed in Sec. III. The figure shows

that $\lambda_L(\epsilon)$ does indeed obey a power law. For $\epsilon > 0.02$, we find $\lambda_L \sim \epsilon^{-0.263\pm0.014}$; for $\epsilon < 0.02$, $\lambda_L \sim \epsilon^{-0.325\pm0.008}$. Since $\epsilon \propto N^{-2}$, these results imply the power-law scaling of $\lambda_L$ with polymerization index $N$ as $\lambda_L \sim N^{\theta}$, where in the weak-segregation regime $\theta_w = 0.526\pm0.028$; in the strong-segregation regime $\theta_s = 0.650\pm0.016$. Our results agree with results from Ohta and Kawasaki's variational calculations[6] and Oono and Bahiana's numerical or dimensional analysis.[9]

We have also done calculations for $f \neq \frac{1}{2}$. In this case, the periodic steady states correspond roughly to the cylindrical or spherical domains observed in uneven block copolymer phase separations. The same scaling exponents $\theta_w = \frac{1}{2}$ and $\theta_s = \frac{2}{3}$ are found.

### C. Scaling hypothesis for block copolymer phase separation

The block copolymer scaling exponents are reminiscent of the asymptotic growth exponents in spinodal decomposition. In veiw of the similarity between the block copolymer and the Cahn-Hilliard equations, it is tempting to seek a connection between the two sets of scaling laws. Specifically, the weak- and strong-segregation regimes may be counterparts of the early and late stages of spinodal decomposition, respectively. Recently, Oono and Bahiana[9] argued that the relationship $\theta = 2\phi$ should hold. Here $\phi$ and $\theta$ are defined by $l(t) \sim t^{\phi}$, $\lambda_L \sim N^{\theta}$. Their arguments are based on the dimensional analysis of the equation of motion of the interface. Results from Sec. II B also seem to support this conclusion.

We now show that the same conclusion can be drawn automatically from a scaling hypothesis for the characteristic length scale of the system. We conjecture that for the block copolymer system, an asymptotic scaling form holds at large $t$ and small $\epsilon$ for the typical length scale of the system $l(t,\epsilon)$,

$$l(t,\epsilon) = \epsilon^{-\theta/2} F(t\epsilon^{\gamma}) , \tag{2.10}$$

where the universal scaling function $F(x)$ satisfies the following properties:

$$F(x) \to \text{const} \quad \text{as } x \to +\infty \tag{2.11a}$$

and

$$F(x) \sim x^{\theta/2\gamma} \quad \text{as } x \to 0 . \tag{2.11b}$$

In the simulations of Ref. 9, $l(t,\epsilon)$ is determined from the wave number at which the spatial Fourier transform of the order parameter has the largest weight.

We assume $\theta, \gamma > 0$. For a given small $\epsilon$, taking the limit $t \to +\infty$ in Eq. (2.10) recovers the lamellar thickness scaling

$$l_{\infty} \equiv l(t \to \infty, \epsilon) = \text{const}\, \epsilon^{-\theta/2} \sim N^{\theta} . \tag{2.12}$$

On the other hand, for large time $t$, the limit $\epsilon \to 0$ gives the spinodal asymptotic scaling

$$l(t, \epsilon \to 0) \sim t^{\theta/2\gamma} . \tag{2.13}$$

Thus $\theta = 2\gamma\phi$. If we assume that the weak-segregation regime in block copolymer corresponds to the surface diffusion-dominated spinodal growth and that the strong-segregation regime corresponds to late-stage spinodal decomposition, as suggested by the results from Sec. II B, Eq. (2.13) gives that $\theta = 2\phi$ and $\gamma = 1$.

To test if the scaling form Eq. (2.10) is indeed true, we need to study the time-dependent behavior of the BCP equation. Unfortunately, direct time-dependent simulations of the BCP equation suffer from the same difficulties as direct simulations of the Cahn-Hilliard equation: they are highly time consuming. The only time-dependent study of the BCP system is that performed by Oono and Bahiana using a computationally efficient two-dimensional cell dynamical system (CDS) approach.[3] Here we use data from the CDS approach in an attempt to check the validity of the scaling hypothesis.

In Fig. 2 we show a graph of $l(t,\epsilon)/l_{\infty}$ versus $t\epsilon$ ($\gamma = 1$) on a log-lot plot. The data points are for $0.002 \le \epsilon \le 0.035$. We observe from Fig. 2 that all data points fall nicely on a single universal curve. The curve goes to a constant at large $t\epsilon$, which is consistent with Eq. (2.11a). The scaling ansatz, Eq. (2.11b), requires the curve to approach a straight line with slope $\theta/2$ as $t\epsilon \to 0$. We see clearly this tendency in Fig. 2 even though more data for small $\epsilon$ are needed to verify the scaling hypothesis convincingly. For the current $\epsilon$ value, we are still in the weak-segregation regime. Supposedly, as $\epsilon \to 0$, the slope will eventually approach $\theta/2 = \frac{1}{3}$.

Our choice of $l_{\infty}$ in Fig. 2 needs some explanation. For $0.006 \le \epsilon \le 0.035$, simulations converge relatively quickly to the final $l_{\infty}$. However, for smaller $\epsilon < 0.006$, due to the finite-size effect, only early time data are avail-

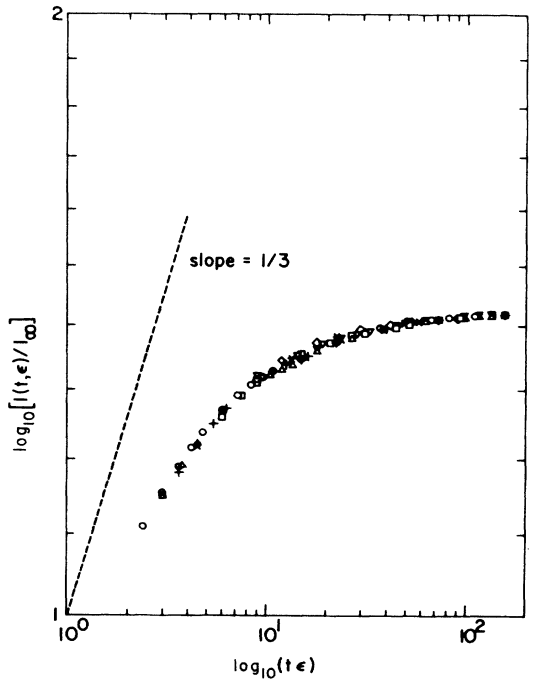


FIG. 2. Scaling of the characteristic length scale from time-dependent cell-dynamical-system simulations. $l(t,\epsilon)/l_{\infty}$ vs $t\epsilon$ in a log-log plot. Data points range from $\epsilon = 0.002$ to 0.035.

able. We write Eq. (2.12) as $l_\infty \sim \epsilon^{-\sigma}$; this scaling is well established[9] for $0.006 \leq \epsilon \leq 0.035$, with $\sigma = 0.254 \pm 0.005$. For this range of $\epsilon$, $l(t,\epsilon)/l_\infty$ is a universal function of $t\epsilon$ with $\sigma \sim 0.259$. For $\epsilon < 0.006$, we simply adjusted $\sigma$ in order that the data would fall on the same universal curve as the data for $0.006 \leq \epsilon \leq 0.035$. The value of $\sigma$ we used was $\sim 0.263$. Note that this is still much smaller than $\frac{1}{3}$, implying that the data are still in the weak-segregation limit.

To summarize, we have proposed a form for the scaling of the dominant length scale, which is supported by cell-dynamical-system time-dependent simulations. Further time-dependent study of the strong segregation regime is required to verify the scaling hypothesis convincingly.

## III. PROPERTIES OF PROPAGATING FRONTS

In this section we study the properties of propagating fronts traveling into the unstable state. When an initially structureless system is rapidly quenched into the homogeneous unstable state and then perturbed locally at some point, the subsequent time evolution is dominated by the motion of a propagating wave front traveling into the unstable state, usually moving with uniform velocity and a well-defined wavelength. This dynamical pattern-selection mechanism has been studied recently[12,13] and has been observed in several systems, e.g., in the Taylor-Couette column[14] and in Rayleigh-Bénard convection.[11]

Our study of the propagating fronts for the block copolymer system is motivated by the observation that the BCP equation is very similar to the Swift-Hohenberg equation,[10] which is a model describing cellular pattern formation in Rayleigh-Bénard convection. The Swift-Hohenberg equation can be written as

$$\frac{\partial \psi(\mathbf{r},t)}{\partial t} = [(\tfrac{1}{4}-\epsilon)-(\nabla^2+\tfrac{1}{2})^2]\psi(\mathbf{r},t)-\psi^3(\mathbf{r},t)$$
$$= -\nabla^4\psi - \nabla^2\psi - \epsilon\psi - \psi^3 , \quad (3.1)$$

where $\epsilon \in [0,\frac{1}{4}]$. The only difference between Eqs. (3.1) and (2.1) is the nonlinear $\psi^3$ term.

The marginal-stability theory[12,13] (MST) has been very successful in studying propagating fronts in many model equations, including the Swift-Hohenberg equation. It is based on a linear stability analysis of the leading edge of the front in the comoving frame of the front. It predicts a unique velocity $c^*$ and wave number $k^*$ for the front:

$$c^* = \frac{\mathrm{Re}\,\omega(\bar{k})}{\mathrm{Im}\,\bar{k}} = -\mathrm{Im}\frac{d\omega(k)}{dk}\bigg|_{\bar{k}}, \quad \mathrm{Re}\frac{d\omega(k)}{dk}\bigg|_{\bar{k}} = 0 , \quad (3.2a)$$

$$k^* = \mathrm{Im}[\omega(\bar{k})/c^* + i\bar{k}] . \quad (3.2b)$$

where $\omega(k) = -k^4 + k^2 - \epsilon$ and $\bar{k}$ is the fastest growing mode in the comoving frame of the front. In the simplest form of the marginal-stability theory, only linear properties of the model equation matter. Note that, in general, the wave number $k^*$ is not the one that minimizes the Lyapunov functional.

The same $c^*(\epsilon), k^*(\epsilon)$ are expected for both the Swift-Hohenberg and the block copolymer equations, since they share the same linear dispersion relation. This is given by

$$c^*(\epsilon) = 4a(1+8a^2), \quad k^*(\epsilon) = \frac{(1+6a^2)^{3/2}}{\sqrt{2}(1+8a^2)} ,$$

where

$$a = (\sqrt{6}/12)[\sqrt{1+6(1-4\epsilon)}-1]^{1/2} .$$

Excellent agreement has been shown[12] for the Swift-Hohenberg equation between the numerically calculated $c^*, k^*$ values and those given by the marginal-stability theory. It is natural to ask how well, if at all, the marginal-stability theory applies to the BCP equation where the nonlinearity is somewhat stronger than that of the Swift-Hohenberg equation.

We integrate Eq. (2.1) numerically in one dimension for a system size $\sim 500$, using the Crank-Nicholson scheme. The system is initially in the unstable $\psi = 0$ state. We trigger a localized perturbation near the origin and monitor disturbances growing into the unstable state. The boundary conditions are $d\psi/dr = d^3\psi/dr^3 = 0$ at two ends. $c^*$ and $k^*$ are measured after the front is sufficiently far away from the initial transients and extrapolation to zero grid spacing is performed to give the final result.

In Fig. 3 we plot the numerically calculated velocity as a function of $\epsilon$; the solid line in the graph is the predic-

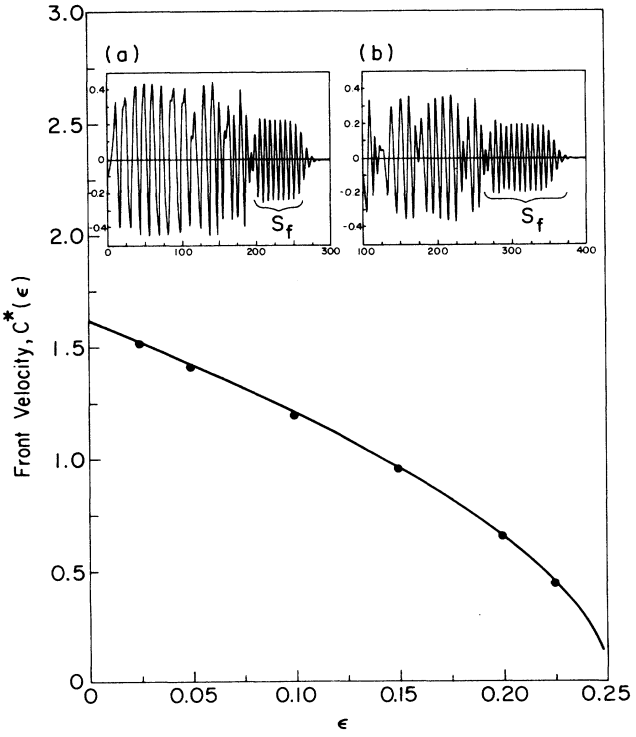


FIG. 3. Front velocity selection $c^*(\epsilon)$. Solid line is the prediction of the marginal-stability theory. Typical patterns of propagating fronts are shown in insets. (a) $\epsilon = 0.025$, $S_f \sim 75$; (b) $\epsilon = 0.1$, $S_f \sim 100$.

tion of the marginal-stability theory. Very good agreement with the theory can be seen over the whole parameter range. However, the spatial pattern looks quite different from that in the Swift-Hohenberg equation. A typical spatial profile consists roughly of two parts (Fig. 3, inset). The first part immediately behind the front consists of regular periodic oscillations of well-defined local wavelength. This "front region" is similar to the front in the Swift-Hohenberg equation. Its size $S_f$ shrinks as $\epsilon$ decreases. Behind this region follows a much more irregular "tail region." The order parameter fluctuates strongly both in amplitude and periodicity. The irregularity is a result of both transients and inherited nonlinearity, most prominently the latter.

We have measured the local wave numbers of the spatial profile. At $\epsilon=0.025$, we find in the front region $k=0.82\pm0.08$, which agrees with the marginal-stability prediction $k^*=0.761$ within numerical accuracy. It is well separated from $k_{\min}=0.381$, which minimizes the free energy. The uncertainty in $k$ here is due mostly to the finite size of the front, since $\delta k\sim 2\pi/S_f$. At the above $\epsilon$ value $S_f\sim 75$ and therefore $\delta k\sim 0.08$. Thus we are unable to distinguish this $k$ from the fastest growing mode $\bar{k}=0.831$. In the tail region the average wave number is found to be $\sim 0.44$, which is very close to $k_{\min}$.

We expect that propagating fronts are observable in real copolymer experiments, especially in the weak-segregation regime, where the front size $S_f$ is relatively large. Due to the complex entanglements of polymer chains, the dynamics is slow, which may assist in the detailed study of various stages of the phase separation process.

To conclude, we have studied a one-dimensional model of the block copolymer phase separation. We demonstrate the existence of a power law scaling of the lamellar thickness with the polymerization index. The scaling exponents are calculated accurately, which supports the previous variational and dimension-analytical results. We have shown that a relation between block copolymer scaling exponents and spinodal decomposition exponents proposed by Oono and Bahiana follows naturally from a scaling form of the typical length scale. Results from Sec. III show that the block copolymer is yet another system where the propagation pattern-selection mechanism is at work and agrees well with the marginal-stability theory.

## ACKNOWLEDGMENTS

We are grateful to Yoshi Oono and Monica Bahiana for kindly providing data from their CDS simulations, and for helpful discussions. We thank the Materials Research Laboratory Center of Computation at the University of Illinois for the use of their facilities. This work was supported by National Science Foundation Grant Nos. NSF-DMR-86-12860 and NSF-DMR-87-01393. N.D.G. gratefully acknowledges the support of the Alfred P. Sloan Foundation and the Center for Advanced Study at the University of Illinois.

[1]H. Furukawa, Adv. Phys. **34**, 703 (1985); J. D. Gunton, M. San Miguel, and P. S. Sahni, in *Phase Transitions and Critical Phenomena,* edited by C. Domb and J. L. Lebowitz (Academic, New York, 1983), Vol. 8.

[2]B. D. Gaulin, S. Spooner, and Y. Morii, Phys. Rev. Lett. **59**, 668 (1987); R. Toral, A. Chakrabarti, and J. D. Gunton, *ibid.* **60**, 2311 (1988); K. Kawasaki and T. Ohta, Physica (Amsterdam) **118A**, 175 (1983); D. Huse, Phys. Rev. B **34**, 7845 (1986).

[3]Y. Oono and S. Puri, Phys. Rev. Lett. **58**, 863 (1987); Phys. Rev. A **38**, 434 (1988).

[4]G. Kämpf, M. Hoffman, and H. Krömer, Ber. Bunsenges. Phys. Chem. **74**, 851 (1970); A. Douy and B. R. Gollot, Mol. Cryst. Liq. Cryst. **14**, 191 (1971).

[5]T. Hashimoto, M. Shibayama, and H. Kawai, Macromolcules **13**, 1237 (1980).

[6]T. Ohta and K. Kawasaki, Macromolecules **19**, 2621 (1986).

[7]L. Leibler, Macromolecules **13**, 1602 (1980).

[8]Y. Oono and Y. Shiwa, Mod. Phys. Lett. B **1**, 49 (1987).

[9]Y. Oono and M. Bahiana, Phys. Rev. Lett. **61**, 1109 (1988).

[10]J. Swift and P. C. Hohenberg, Phys. Rev. A **15**, 319 (1977).

[11]J. Fineberg and V. Steinberg, Phys. Rev. Lett. **58**, 1332 (1987).

[12]G. Dee and J. S. Langer, Phys. Rev. Lett. **50**, 383 (1983); E. Ben-Jacob, H. Brand, G. Dee, L. Kramer, and J. S. Langer, Physica **14D**, 348 (1985).

[13]W. van Saarloos, Phys. Rev. Lett. **58**, 2571 (1987); Phys. Rev. A **37**, 211 (1988).

[14]G. Ahlers and D. S. Cannell, Phys. Rev. Lett. **50**, 1583 (1983); M. Lücke, M. Mihelcic, and K. Wingerath, *ibid.* **52**, 625 (1984), Phys. Rev. A **31**, 396 (1985).